Dynamical Structure Factor of the Three-Dimensional Quantum Spin Liquid Candidate NaCaNi_{2}F_{7}

Shu Zhang, Hitesh J. Changlani, Kemp W. Plumb, Oleg Tchernyshyov, and Roderich Moessner

Dynamical structure factor of the three-dimensional quantum spin liquid candidate NaCaNi$_2$F$_7$

Shu Zhang,[1,2] Hitesh J. Changlani,[3,1,2] Kemp W. Plumb,[4] Oleg Tchernyshyov,[1,2] and Roderich Moessner[5]

[1]*Department of Physics and Astronomy, Johns Hopkins University, Baltimore, MD 21218*
[2]*Institute for Quantum Matter, Johns Hopkins University, Baltimore, MD 21218*
[3]*Department of Physics, Florida State University, Tallahassee, Florida 32306*
[4]*Department of Physics, Brown University, Providence, RI 02912*
[5]*Max-Planck Institute for the Physics of Complex Systems, 01187 Dresden, Germany*
(Dated: March 29, 2019)

We study the dynamical structure factor of the spin-1 pyrochlore material NaCaNi$_2$F$_7$, which is well described by a weakly perturbed nearest-neighbour Heisenberg Hamiltonian, Our three approaches—molecular dynamics simulations, stochastic dynamical theory and linear spin wave theory—reproduce remarkably well the momentum dependence of the experimental inelastic neutron scattering intensity as well as its energy dependence with the exception of the lowest energies. We discuss two surprising aspects and their implications for quantum spin liquids in general: the complete lack of sharp quasiparticle excitations in momentum space and the success of the linear spin wave theory in a regime where it would be expected to fail for several reasons.

Quantum spin liquids (QSLs) [1] are enigmatic phases of matter characterized by the absence of symmetry breaking and conventional quasiparticles (magnons). The search for QSLs in actual magnetic materials has targeted materials with low spin and geometric frustration [2]. Indeed, while there have been significant efforts to synthesize quantum spin liquid materials in spin-1/2 systems in two dimensions, fewer efforts have been devoted to three dimensions, for a review see Ref. [3]. This strategic choice is not without reason: higher spin and number of dimensions typically suppress quantum fluctuations and favor magnetically ordered states over QSLs. However, it is now clear that this perspective is too pessimistic: we know that certain types of spin liquid can exist in $d = 3$ but not in $d = 2$ [4, 5]. Therefore QSLs need not be restricted to $d = 2$ and $S = 1/2$ exclusively [6–8].

Despite some recent advances, our understanding of low-spin Heisenberg QSLs in three dimension limited as they are often beyond the scope of exact or controlled approximate theoretical schemes. We are at a loss to describe either their ground states or excitation spectra, unlike Ising models like spin ice, where the simplest quantum versions [4, 5] are amenable to quantum Monte Carlo (QMC) simulations [9, 10]. Experiments are therefore an indispensable guide for our understanding of these magnets [11].

The quest for QSLs relies heavily on characteristic signatures in the excitation spectra: while QSL ground states are often largely featureless, their excitations can be quite unusual, including in particular fractionalized [12, 13] quasiparticles such as spinons in the spin-1/2 Heisenberg antiferromagnetic chain [14–16], Majorana fermions in the Kitaev honeycomb model [17–19], and photons in the U(1) spin liquid [4, 5, 10].

The dual challenge is thus to identify novel phenomena in experimental data and to devise a theoretical framework for understanding the underlying behavior. Here we report progress for the fluoride pyrochlore NaCaNi$_2$F$_7$ [20]. Its magnetic Ni^{2+} ions have spin $S = 1$ and reside on the three-dimensional pyrochlore lattice (Fig. 1). Strong geometrical frustration and short spin length may produce a QSL [7, 21].

We analyze the magnetic excitation spectrum [22], including new, hitherto unpublished data. Our three complementary theoretical approaches reproduce the dynamical struc-
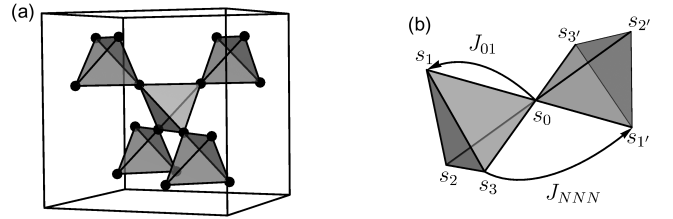

Figure 1. (a). Pyrochlore lattice in one cubic unit cell. (b). Nearest-neighbor and next-nearest-neighbor interactions.

ture factor $\mathcal{S}(\mathbf{q}, \omega)$ for all momenta $\mathbf{q}$ and for a broad range of energies ω; the quality of the agreement differs between methods at the highest energies. At low energies, we find the well-known pinch-point motifs; at intermediate energies, characteristic structures complementary to the pinch points appear [23, 24]. Overall, the main disagreement between experiment and theory appears at the lowest energies, as discussed below.

Given the abovementioned challenges in $d = 3$, the success of our relatively simple approaches is as striking as it is encouraging. We therefore include a discussion of the broader implications of our results about the nature of quantum spin liquid dynamics, which we believe is applicable more broadly.

We emphasize that none of our theoretical approaches relies on the existence of magnons or other quasiparticles with well-defined momentum $\mathbf{q}$ and energy ω, nor do they require the presence of delicate quantum coherence. Nonetheless, even *linear spin wave theory* is successful in this context!

The main results are presented as a comparison of scattering intensity for NaCaNi$_2$F$_7$ as a function of momentum (Fig. 2) and energy (Figs. 3, 4). For the methodologically interested reader, we collate all technical information in a set of self-contained appendices [26].

Model and methods: We use the Hamiltonian (Fig. 1)

$$H = \frac{1}{2} \sum_{ij} \sum_{\mu\nu} J_{ij}^{\mu\nu} s_i^\mu s_j^\nu, \tag{1}$$
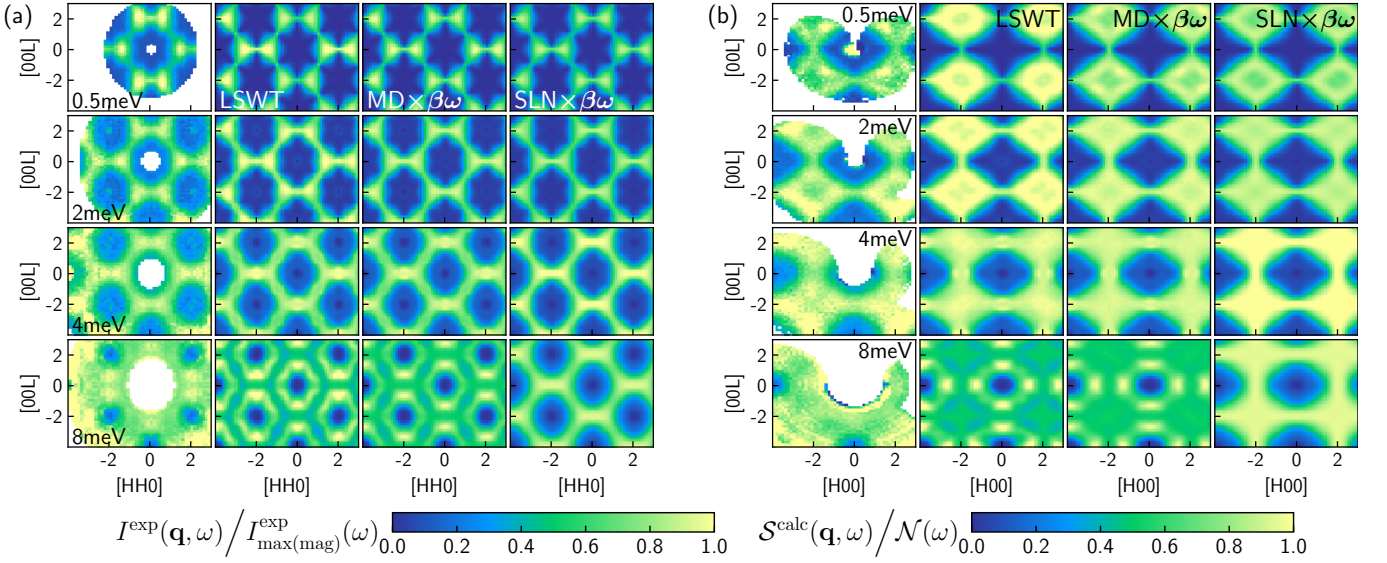
Figure 2. (Color) Dynamical structure factor in (a) [HHL] and (b) [H0L] planes at constant energies: experiment compared to linear spin wave theory, molecular dynamics, and the stochastic model. Data in (a) were collected on CNCS and in (b) on MACS. Raw neutron intensity has been corrected by the magnetic form-factor for Ni^{2+} [25]. To focus on wavevector dependence, data are rescaled for each value of energy, for experiment, by the maximum magnetic scattering intensity; and by the maximum intensity in the MD simulations for the six theory panels, with an additional factor $\beta\omega$ between MD/SLN and LSWT (Eq. (21) in [26], see text), $\mathcal{N}(\omega) = \beta\omega\mathcal{S}_{max}^{MD}(\omega)$, where $\beta = 1/k_BT$.

where Roman subscripts refer to lattice sites and Greek superscripts to Cartesian spin components. The interaction matrix $J_{ij}^{\mu\nu}$ [30] is parameterized by four exchange parameters $J_{01} = (J_2, J_4, J_4; -J_4, J_1, J_3; -J_4, J_3, J_1)$ with $J_1 = J_2 = 3.2(1)$ meV, $J_3 = 0.019(3)$ meV, $J_4 = -0.070(4)$ meV for nearest neighbors. The interaction matrices for other pairs follow from appropriate symmetry transformations. These parameters and Heisenberg exchange for next-nearest-neighbors $J_{NNN} = -0.025(5)$ meV were previously extracted by some of us from equal-time correlations [22].

The three methods utilized are: firstly, molecular dynamics (MD) simulations of the pyrochlore magnet [31], where the classical Landau-Lifshitz equations of motion for the spins are integrated numerically and averaged over initial conditions obtained from Monte Carlo simulations at temperature $T = 1.8$ K; secondly, linear spin-wave theory (LSWT) to describe spin dynamics near a low-energy state with a similar averaging over initial conditions; thirdly, a self-consistent Gaussian approximation adapted to frustrated magnets [32] and extended into a stochastic model by Conlon and Chalker [33], which we refer to as stochastic large-N (SLN). See Supplementary Material [26] for details.

The central object of investigation are the dynamical spin correlations, whose Fourier transform is the structure factor

$$\mathcal{S}(\mathbf{q}, \omega) = \sum_{\mu\nu} (\delta_{\mu\nu} - \frac{q_\mu q_\nu}{q^2})$$
$$\times \frac{1}{2\pi N} \sum_{i,j=1}^{N} \int_{-\infty}^{\infty} dt\, e^{-i\mathbf{q}\cdot(\mathbf{r}_i - \mathbf{r}_j) + i\omega t} \langle s_i^\mu(t) s_j^\nu(0)\rangle.$$
(2)

The classical expression is given above and the quantum expression is sensitive to time order of the spin operators [26].

Throughout this work, we rescale the two "classical" approaches MD and SLN by $\omega/(k_BT)$ to make comparison with LSWT. This factor crudely reproduces the effects of quantum fluctuations at low temperatures [26].

Results: $\mathcal{S}(\mathbf{q}, \omega)$ obtained experimentally and by the three theories is depicted as a function of wavevector $\mathbf{q}$ in a set of cuts at various energies, Fig. 2, and as a function of energy ω along a set of paths through reciprocal space, Fig. 3.

Fig. 2 displays normalized structure factor along momentum cuts in the [HHL] and [H0L] planes at energies $\omega = 0.5$, 2, 4 and 8 meV. At low energies, the pinch points characteristic of a U(1) spin liquid are clearly visible. Their presence implies that each tetrahedron has vanishing total magnetization [34, 35]. In general, however, adjacent tetrahedra cannot both be in $S = 0$ states, as their total spin operators do not commute. Therefore, while for the classical theories, the pinch points sharpen as $\sqrt{T}$ as T is lowered [36], for $S = 1/2$ they were found to be quite smeared out [21], becoming sharper as S increases. For $S = 1$, a prediction for the full-width at half maximum of the pinch point in the static correlations at [002] of $\delta q_{PP}^{FWHM} = 4\pi/3$ [7] is comparable to the value $\approx \pi$ extracted form the low-T experimental data.

As the energy increases, the overall intensity distribution changes little initially, but what sharp features were present wash out; e.g., the intensity minimum in the scattering rhombus around [202] is slowly filled in and the pinch points broaden. At higher energies, phonons pollute the experimental signal at large $\mathbf{q}$, but a rearrangement of the weight is still discernible, with the area around the pinch-points growing into prominent pairs of "half-moons" features at 8 meV, a dispersing complement to the pinch points [23, 24]. This feature is present in MD and LSWT, but not in SLN, which is relaxational and does not capture spin precession.

We next turn to the energy dependence of the data, Fig. 3, with additional data from a different neutron instrument [26], Fig. 4. The general shapes of experiment and MD/LSWT are very similar—a broad signal with a vertical appearance reminiscent of a fountain. SLN fails to capture the high-energy structure, which can therefore be ascribed to the precessional spin dynamics not captured by this method; otherwise, the theory plots agree with one another.

The largest disagreement between theory and experiment occurs at low frequencies, especially around [220], where a large increase of the experimental signal below 1 meV is not reflected in theory, Fig. 4. More on that below.
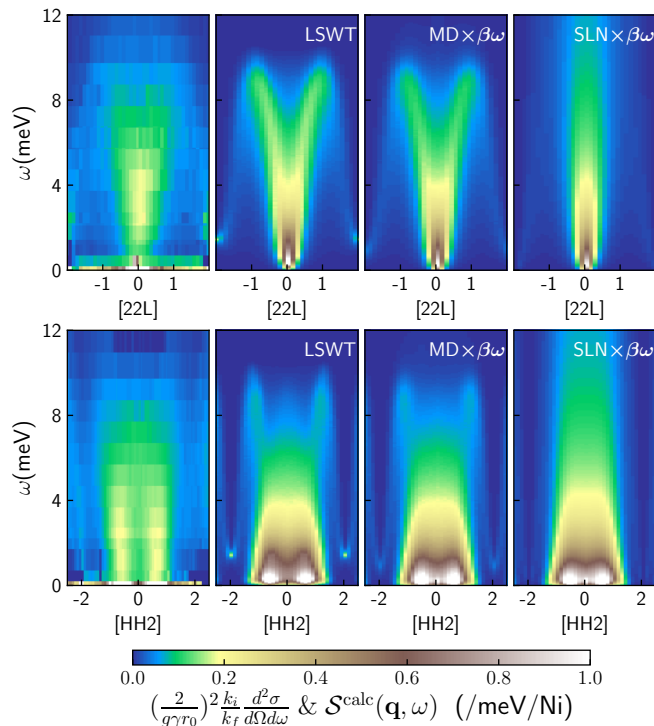

Figure 3. (Color) Energy dependence of dynamical structure factor along momentum cuts [22L] and [HH2]. Neutron scattering intensity is in absolute units [26]. Rescaled MD and LSWT in particular reproduce well the shape of the broad dispersive curve, disagreeing mainly at the lowest energies; SLN fails to capture high-energy structure.

Discussion: We next address the remarkable agreement between theory and experiment (with the exception of the lowest energies) on the one hand and between MD and LSWT on the other. The latter is quite unexpected: there, after all, are several reasons why LSWT should break down in a $S=1$ Heisenberg pyrochlore antiferromagnet. Instead, it works unreasonably well, as detailed above. The inauspicious ingredients are, firstly, absence of a state with long-range order around which to perturb, the existence of which would have guaranteed a Goldstone mode as long-lived magnon excitation. Other models without long-range order, such as the $S=1/2$ and 1 Heisenberg chains, instead show a breakdown of LSWT, as their respective low-energy descriptions involve not the gapless magnons but either fractionalized $S=1/2$ spinons or Haldane's gap. Secondly, the spin length $S=1$ really is small, so
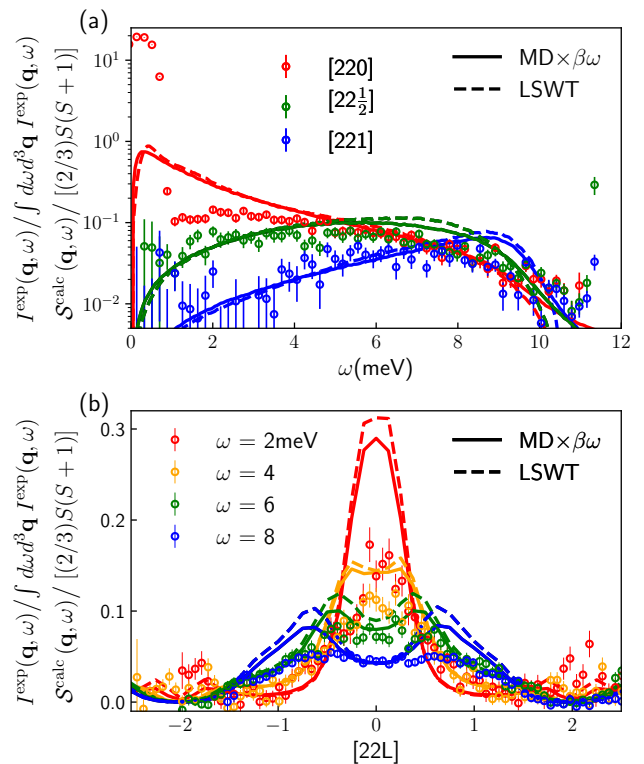

Figure 4. (Color) Comparison of dynamical structure factor between experiment and MD/LSWT. (a) Energy-dependence at $\mathbf{q} =$ [220], [22$\frac{1}{2}$] and [221]. Log scale is used for the y-axis to include the quasi-elastic signals. (b) Momentum dependence along [22L] at $\omega = 2,4,6$ and 8meV. The neutron scattering intensity $I^{\mathrm{exp}}(\mathbf{q},\omega)$ is background subtracted and normalized by the total spectral weight $\int d\omega d^3\mathbf{q}\, I^{\mathrm{exp}}(\mathbf{q},\omega)$. MD (solid lines) and LSWT (dashed lines) data $\mathcal{S}^{\mathrm{calc}}(\mathbf{q},\omega)$ are normalized by $(2/3)S(S+1)$, under an isotropic approximation to the sum rule.

that one might expect considerable quantum renormalization effects, all the more so since the classical local exchange field is reduced as a result of geometric frustration from $6S$ in a ferromagnet to $2S$. Finally, a finite fraction of the spin-wave modes live at or near zero energy in LSWT, which implies the onset of the many-particle continuum *already at the bottom of the single-particle spectrum.* Above this onset, spin waves are expected to show damping [37].

LSWT actually finds another route to work: it is not a theory of universal low-energy hydrodynamic excitations, but of the statistically typical behavior at short time/high energies scales, which fails at long times/low energies, thus in the end conforming to at least a subset of the above expectations.

To see this, think of the (near-)zero frequency modes as responsible for "slow" motion between (near-)degenerate ground states, and of "fast" oscillatory spin waves—with finite frequency and scattering rates—around these as driving this motion [31, 33, 38]. *Statistically,* the spectra of these fast oscillations appear not to change as the slow modes evolve, making the broad finite-frequency spectra we consider here effectively time-independent. Indeed, we do find self-averaging in practice as only a few configurations are needed to obtain smooth spectra for large system sizes [26], in keep-

ing with the observation that disorder is weak in that it occurs mainly in off-diagonal terms of the dynamical matrix, with the diagonal exchange field nearly uniform. As expected for weak disorder in three dimensions, spin waves away from the band edges are delocalized, as diagnosed by the scaling of their inverse participation ratio with the system size, see [26].

This also explains why spin-wave scattering does not invalidate the picture: LSWT predicts a broad continuum in frequency space to begin with, and any further broadening of an individual mode due to its finite lifetime is small in temperature T, and therefore parametrically smaller than the total (largely T-independent) bandwidth. Thus, unlike in the case of an initially sharp mode, lifetime broadening is insignificant.

In the low-T limit, zero modes have no dynamics in LSWT (their frequency is zero). Motion along the ground-state manifold is thus frozen out and LSWT fails to capture their motion arising from scattering off high-energy excitations, which is present in MD and SLN theories. It is thus clear that our comparison is not particularly sensitive to the details of the low-frequency physics.

Typically, the universal low-energy features of spin liquid ground states are topological in nature and as such invisible to experimental probes that couple to local correlations [39]. Indeed, it has been a common recent theme in quantum magnets that the structure factor *away from* low energies is most instructive. While this part of the spectrum is not universal, and may not contain enough information to pin down the nature of the quantum spin liquid unambiguously, it permits simple modeling and detailed comparison with experiments (e.g., of deconfined spinons for weakly coupled Heisenberg chains [15]). Furthermore, the presence of disorder and freezing [20, 40] likely renders the low-energy features fragile, thus requiring additional modeling [41]. More generally, further small terms in the Hamiltonian, potentially missed by our fitting procedure, may redistribute low-energy spectral weight, and even lead to a conventional ordered state at the lowest termperatures; in this case, the modelling presented here applies to the proximate spin liquid regime at temperatures/energies above the small transition energy scale. Finally, an accurate treatment of low-energy features requires going beyond the simple version of our classical-quantum correspondence factor $\beta\omega$.

All these complications should not distract from an important feature seen in experiment and reproduced in theory: the complete absence of sharp quasiparticle peaks characteristic of magnons with well-defined momenta and energies. It reflects the spatially disordered nature of the spin configurations in our classical theory and raises the question about the appropriate description of the corresponding low-temperature quantum state. An interesting scenario is that small-spin pyrochlore Heisenberg antiferromagnets exhibit no well-defined quasiparticle excitations at all.

The final basic issue raised by our study is the role of the "quantumness" in this compound. The relative success of fully classical modeling across a broad range of energies, at temperatures far below the Curie-Weiss scale, is rather unexpected. The low-energy discrepancies discussed above seem like a small price to pay for the huge simplicity of our theoretical approaches. This calls for experiments on analogous compounds with larger spins, to investigate whether the low-energy regime will be better modeled while retaining the other features already successfully accounted for.

Employing semi-classical modelling for what is expected to be a quantum spin liquid is not without precedent. This was done for the Kitaev honeycomb model [17], whose exact solvability allows for a reliable comparison in detail [42]. There [43], the high-frequency portion of the response was accounted for modulo a reasonable amount of data post-processing, while the physics related to the emergent fluxes at low energies—the most direct manifestation of fractionalization—remained inaccessible.

Similarly, qualitative signatures of a quantum spin liquid may be visible only at the lowest energies. If so, the challenge is to explain a rapid crossover into a classical regime, where quantum mechanics mainly enters in the mode occupation numbers. An alternative would be the absence of a qualitatively distinct low-frequency quantum spin liquid regime altogether. This could either happen intrinsically, if the emergent low-energy description is amenable to a semi-classical description; or extrinsically, in that the quantum spin liquid behavior is so fragile that disorder or coupling to phonons destroy it entirely. It would be worthwhile to examine materials with other values of spin (and preferably free from quenched disorder) and to explore the low-energy behavior.

Note: Shortly after we posted the present work on the arXiv, another preprint by Bai *et al.* [44] appeared there, which presents a closely related study with similar conclusions on the $S = 3/2$ spinel compound $MgCr_2O_4$.

[1] P. W. Anderson, Mater. Res. Bull. **8**, 153 (1973).

[2] C. Lacroix, P. Mendels, and F. Mila, *Introduction to Frustrated Magnetism* (Springer, Berlin, Heidelberg, 2011).

[3] Y. Zhou, K. Kanoda, and T.-K. Ng, Rev. Mod. Phys. **89**, 025003 (2017).

[4] R. Moessner and S. L. Sondhi, Phys. Rev. B **68**, 184512 (2003).

[5] M. Hermele, M. P. A. Fisher, and L. Balents, Phys. Rev. B **69**, 064404 (2004).

[6] F.-Y. Li and G. Chen, Phys. Rev. B **98**, 045109 (2018).

[7] Y. Iqbal, T. Müller, P. Ghosh, M. J. P. Gingras, H. O. Jeschke, S. Rachel, J. Reuther, and R. Thomale, arXiv:1802.09546.

[8] T. Fennell, M. J. Harris, S. Calder, M. Ruminy, M. Boehm, P. Steffens, M. H. Lemée-Cailleau, O. Zaharko, A. Cervellino, and S. T. Bramwell, Nat. Phys. (2018), 10.1038/s41567-018-0309-3.

[9] A. Banerjee, S. V. Isakov, K. Damle, and Y. B. Kim, Phys. Rev. Lett. **100**, 047208 (2008).

[10] O. Benton, O. Sikora, and N. Shannon, Phys. Rev. B **86**, 075154 (2012).

[11] M. J. Harris and M. P. Zinkin, Mod. Phys. Lett. B **10**, 417 (1996).

[12] R. Rajaraman, "Fractional charge," in *Quantum [Un]speakables: From Bell to Quantum Information* (Springer, Berlin, Heidelberg, 2002) pp. 383–399.

[13] L. Savary and L. Balents, Rep. Prog. Phys. **80**, 016502 (2017).

[14] H. Bethe, Z. Physik **71**, 205 (1931).

[15] B. Lake, D. A. Tennant, J.-S. Caux, T. Barthel, U. Schollwöck, S. E. Nagler, and C. D. Frost, Phys. Rev. Lett. **111**, 137205 (2013).

[16] M. Mourigal, M. Enderle, A. Klöpperpieper, J.-S. Caux, A. Stunault, and H. M. Ronnow, Nat. Phys. **9**, 435 (2013).

[17] A. Kitaev, Ann. Phys. **321**, 2 (2006).

[18] A. Banerjee, J. Yan, J. Knolle, C. A. Bridges, M. B. Stone, M. D. Lumsden, D. G. Mandrus, D. A. Tennant, R. Moessner, and S. E. Nagler, Science **356**, 1055 (2017).

[19] Y. Kasahara, T. Ohnishi, Y. Mizukami, O. Tanaka, S. Ma, K. Sugii, N. Kurita, H. Tanaka, J. Nasu, Y. Motome, T. Shibauchi, and Y. Matsuda, Nature **559**, 227 (2018).

[20] J. W. Krizan and R. J. Cava, Phys. Rev. B **92**, 014406 (2015).

[21] B. Canals and C. Lacroix, Phys. Rev. Lett. **80**, 2933 (1998).

[22] K. W. Plumb, H. J. Changlani, A. Scheie, S. Zhang, J. W. Krizan, J. A. Rodriguez-Rivera, Y. Qiu, B. Winn, R. J. Cava, and C. L. Broholm, Nat. Phys. (2018), 10.1038/s41567-018-0317-3.

[23] H. Yan, R. Pohle, and N. Shannon, arXiv:1806.08520.

[24] T. Mizouguchi, L. D. C. Jaubert, and M. Udagawa,

[25] P. J. Brown, *International Tables for Crystallography*, Vol. C (Springer, Berlin, Heidelberg, 2006) Chap. 4.4.5, pp. 454 –461.

[26] Supplementary Material, which includes Refs.[27-29].

[27] A. G. D. Maestro and M. J. P. Gingras, J. Phys. Condens. Matter **16**, 3339 (2004).

[28] L. R. Walker and R. E. Walstedt, Phys. Rev. B **22**, 3816 (1980).

[29] H. Yamaguchi, K. Katsumata, M. Hagiwara, M. Tokunaga, H. L. Liu, A. Zibold, D. B. Tanner, and Y. J. Wang, Phys. Rev. B **59**, 6021 (1999).

[30] K. A. Ross, L. Savary, B. D. Gaulin, and L. Balents, Phys. Rev. X **1**, 021002 (2011).

[31] R. Moessner and J. T. Chalker, Phys. Rev. Lett. **80**, 2929 (1998).

[32] D. A. Garanin and B. Canals, Phys. Rev. B **59**, 443 (1999).

[33] P. H. Conlon and J. T. Chalker, Phys. Rev. Lett. **102**, 237206 (2009).

[34] S. V. Isakov, K. Gregor, R. Moessner, and S. L. Sondhi, Phys. Rev. Lett. **93**, 167204 (2004).

[35] C. L. Henley, Annu. Rev. Condens. Matter Phys. **1**, 179 (2010).

[36] M. P. Zinkin, Ph.D. thesis, University of Oxford (1996).

[37] A. L. Chernyshev and M. E. Zhitomirsky, Phys. Rev. B **79**, 144416 (2009).

[38] R. Moessner and J. T. Chalker, Phys. Rev. B **58**, 12049 (1998).

[39] J. Knolle and R. Moessner, arXiv:1804.02037.

[40] Y. Cai, M. N. Wilson, A. M. Hallas, L. Liu, B. A. Frandsen, S. R. Dunsiger, J. W. Krizan, R. J. Cava, O. Rubel, Y. J. Uemura, and G. M. Luke, arXiv:1806.10970.

[41] T. E. Saunders and J. T. Chalker, Phys. Rev. Lett. **98**, 157201 (2007).

[42] J. Knolle, D. L. Kovrizhin, J. T. Chalker, and R. Moessner, Phys. Rev. Lett. **112**, 207203 (2014).

[43] A. M. Samarakoon, A. Banerjee, S.-S. Zhang, Y. Kamiya, S. E. Nagler, D. A. Tennant, S.-H. Lee, and C. D. Batista, Phys. Rev. B **96**, 134408 (2017).

[44] X. Bai, J. A. M. Paddison, E. Kapit, S. M. Koohpayeh, J.-J. Wen, S. E. Dutton, A. T. Savici, A. I. Kolesnikov, G. E. Granroth, C. L. Broholm, J. T. Chalker, and M. Mourigal, arXiv:1810.11869.

arxiv:1806.08534.